Automatic Light Intensity Modulation Using TNCbased Artificial Iris for Smart Contact Lens

Adwait Deshpande*, Chayanjit Ghosh*, Mohit U. Karkhanis, Aishwaryadev Banerjee, Erfan Pourshaban, Md. Rabiul Hasan, Amirali Nikeghbal, Md. Golam Dastgir, Hanseup Kim, and Carlos H. Mastrangelo Department of Electrical and Computer Engineering, The University of Utah, Salt Lake City, Utah, USA adwait.p.deshpande@utah.edu *Equal contributing authors

Abstract—In this paper we propose an artificial iris to tackle photophobia. This artificial iris is made with a twisted nematic cell (TNC) sandwiched between two linear polarizers. The light attenuation performance of a commercial TNC was compared with TNCs made from 5CB and E7 liquid crystals (LC) over a standard digital voltage range of 0 to 5V, automatically controlled by a light dependent resistor (LDR). The 5CB-based TNC exhibited lower threshold voltage than commercial TNC and entire light attenuation range around 3.3V, making it compatible with low-power electronic platforms. Maximum light attenuation equivalent to that of a ND32 filter was achieved. Utilizing polarizers in cross-plane or in-plane configuration, photophobia mitigation can be achieved in outdoor and indoor environment, while minimizing power consumption.

Keywords—artificial iris; photophobia; smart contact lens; light intensity modulation; twisted nematic cell

I. INTRODUCTION

Photophobia is a misnomer, meaning fear of light. Lebensohn defined photophobia as an abnormal sensitivity to light. This sensory disturbance provoked by light could cause uncomfortable vision or induce or exacerbate pain [1]. Conditions associated with photophobia can be broadly classified into ophthalmologic disorders, neurological disorders, psychiatric disorders, or drug-induced photophobia [2]. Migraine is the most common disorder causing photophobia [3]. Approximately 80% of the people affected by migraine are affected by photophobia [4]. It is also seen that light can trigger between 30 to 60% of all migraine attacks [5]. Another cause of photophobia is a genetic disorder called aniridia. The pupil regulates the amount of light entering the eye. The iris is responsible for the dilation and constriction of the pupil in lowlight and bright-light environments. Aniridia is a condition in which a person's iris is either partially or entirely missing [6]. In all these cases, patients complain of discomfort in lighting, which can be normal for others, such as natural sunlight, fluorescent lights, etc. [7]. Photophobia is almost always a symptom of some underlying condition. Hence, it can be mitigated once the underlying condition is cured. Presently, a complete cure for migraine and aniridia is unavailable. Photophobia is thus not completely curable in these cases, and hence the discomfort caused because of it has to be alleviated [8]. Reducing the amount of light entering the eye is the most commonly used method to tackle photophobia. Some optical tints have been successful in tackling photophobia. FL-41, a rose-colored tint, was found to increase the discomfort threshold

[9]. It filters out about 80% of the flicker found in fluorescent lighting. Several other tint colors have been tried in literature. However, a significant difference in light tolerance threshold was not observed between FL-41 and gray tints [10]. Along with filters, artificial iris incorporated in eyeglasses, intraocular lenses, and contact lens have been used to reduce photophobia [11]–[13]. The breakthroughs in smart contact lens technologies has been made possible through advancements in miniaturized, soft, stretchable systems [14], [15]. This facilitated integration of a variety of vital components like object distance rangers [16]–[18], energy harvesters [19]–[24], and liquid crystal (LC) lens [25]-[27] onto flexible contact lens platforms. A noninvasive, artificial iris integrated into a smart contact lens system could ideally modulate the ambient light to suit the needs of a person with photophobia. Guest-host liquid crystal-based artificial iris was developed earlier [28]. Here, the artificial iris was made of concentric electrodes. Each section could be turned on or off by applying voltage, thus effectively reducing the pupil diameter. However, at a set pupil diameter, it does not allow for modulating the intensity of light incident on the pupil. In this paper, we propose a novel structure of artificial iris where a twisted nematic cell (TNC) is sandwiched between two linear polarizers, either in-plane or cross-plane. Depending on the polarization configuration, light can be attenuated when a voltage is applied or vice versa. A light dependent resistor senses the amount of ambient light and automatically adjusts the attenuation level.

II. WORKING PRINCIPLE

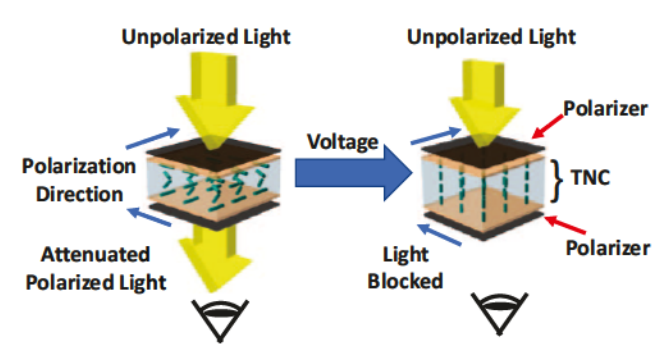


Fig. 1. Ideal working principle of the Polarizer-TNC-Polarizer, artificial iris stack for cross-polarization configuration.

The working of a Polarizer-TNC-Polarizer artificial iris stack is shown in Fig. 1. The polyimide alignment layers on ITO-coated glass are rubbed parallel to the glass surface and then assembled orthogonally. This causes the LC to adopt a

This research was performed under NSF CPS grant 10053422

twisted state [29]. The TNC thus behaves as a polarization rotator. It rotates the polarization of the light on the application of an external AC voltage. This assembly is then placed between two orthogonally placed linear polarizer films. Without the TNC, a cross-polarizer configuration should block the light. However, when a TNC is introduced between two crosspolarized films, due to the twisted nature of the liquid crystals and their birefringence property, the polarization of the light ideally changes by 90 degrees. Thus, all the incoming light is passed through the assembly. When a voltage above the threshold voltage is applied between the two glass plates, the generated electric field causes the liquid crystals to start to lose their twisted arrangement, and the assembly starts getting darker. When the voltage is increased beyond a saturation point, the liquid crystals become perpendicular to the glass plates, ideally resulting in complete light attenuation [30], [31]. For cross-polarizers, the voltage-dependent optical transmission factor is given by (1), where Θ is the twist angle of the cell, $\Delta \phi$ is the phase retardation acquired by the LC and U = $\pi d\Delta n/(\lambda\theta)$ [31].

$$T = \left(1 - \frac{\sin^2\left[\Theta(1 + U^2)^{\frac{1}{2}}\right]}{(1 + U^2)}\right) \cdot \left(1 - \sin^2 2\psi \cdot \sin^2 \frac{\Delta\phi}{2}\right) \tag{1}$$

III. DEVICE STRUCTURE

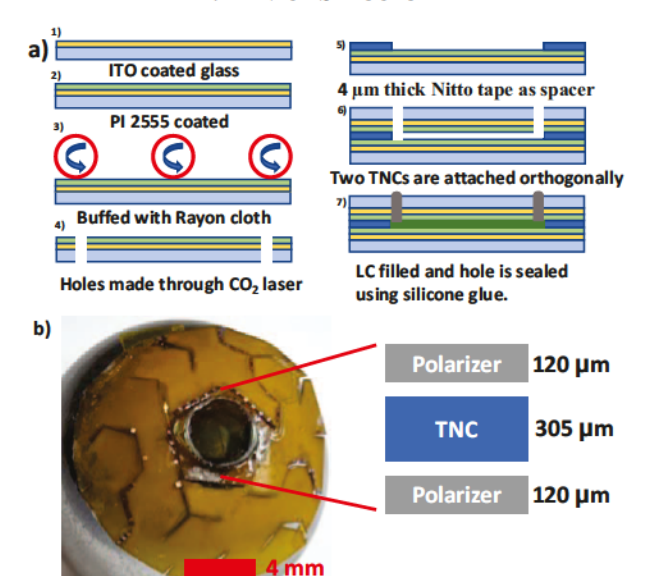


Fig. 2. (a) Fabrication process flow of TNC. (b) Artificial iris stack on flexible, smart contact lens platform.

The TNC was constructed using a simple parallel plate chamber filled with 5CB liquid crystal material. A thin layer of ITO (~200 nm) is deposited using DC sputtering in a 2% oxygen environment. Then we spin-coated a 1:2 solution of Polyimide PI 2555 and N-Methylpyrrolidone (NMP) by weight on the ITO-coated substrate at 4000 RPM for 60 seconds. The sample was soft-baked at 90°C and 100°C for 1 minute each and then baked at 300°C for 3 hours in a nitrogen-rich environment. The post-curing thickness of the polyimide layer is about ~ 50 nm. A thin polyimide layer ensures a low threshold switching voltage for the twisted nematic cell. After curing, we etch part of the polyimide using oxygen plasma and deposit a thin layer

of copper (~200 nm) on the ITO for improved electrical connectivity. After that, the polyimide-coated ITO layer was softly rubbed with a rayon cloth-covered roller. This process aims to provide an initial ~0° LC director tilt alignment. The thin PI layer is susceptible to scratching and peeling off while rubbing. Hence, after the buffing process, the sample was inspected under a high-resolution optical microscope (Keyence VHX 5000) to ensure the polyimide on the ITO's surface was intact and continuous. Using a carbon dioxide laser, we assemble the TNC by cutting glass coverslips into the required shape. We also make two holes ($\sim 100 \mu m$) on one of the glass substrates for LC injection, arrange them orthogonally with respect to the rubbing direction and attach them with a ~4 µm thick double-sided tape (Nitto Denko 5600). This tape also acts as a uniform spacer for the TNC chamber. The orthogonal alignment of the buffing direction is critical for the TNC application. The exposed copper-coated part of the TNC is attached with flex PCB using a conductive polymer (MG Chemicals 9410) and cured at 90°C for 30 minutes to form a conductive path between the TNC and the flex PCB. The TNC (attached with flex PCB) is then vacuum filled in a desiccator attached to a vacuum pump. A droplet of of the LC is dropped on the holes on the glass substrate and vacuum filled. The liquid crystal fills into the chamber of the TNC because of capillary effect. The holes on the TNC are then sealed with silicone glue. The holes are outside the optical aperture for the contact lens, and hence they do not interfere with the wearer's vision. After this process, we attach two linear polarizers (American Polarizers, S-AP42-005T-PSA-12aX19) in cross-plane or inplane arrangement on either side of the TNC on the flexible PCB. The fabrication process flow is shown in Fig. 2. (a). Fig. 2. (b) shows the artificial iris stack on a smart contact lens platform.

IV. SETUP AND EXPERIMENTS

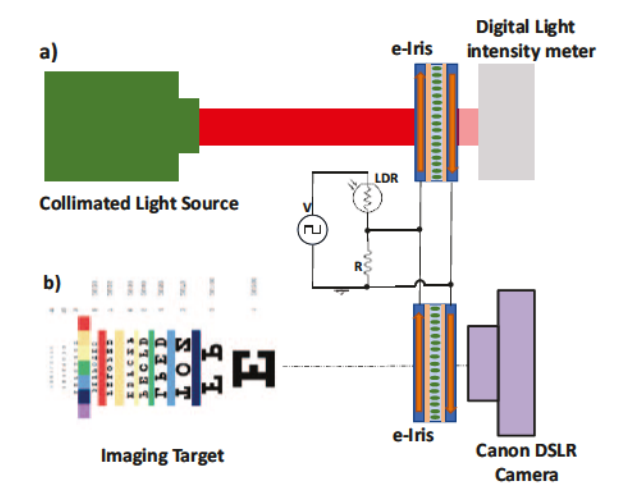


Fig. 3. (a) Experimental setup to measure the light intensity. (b) Setup for imaging target through the artificial iris.

Two different setups were built. One measured the transmitted light intensity through the artificial iris, as shown in Fig. 3. (a), and the other was for imaging a target through the iris, shown in Fig. 3. (b). To measure the intensity of the light, we used a 625 nm wavelength collimated LED light source (M625L3-C1). The light source is placed at a distance of 144 cm

from the artificial iris stack, and the modulated light intensity is measured using a light intensity meter (LX 1330B). Using an Arduino, we supplied a 5V, 1kHz square wave signal with 50% duty cycle, to a voltage divider circuit. One arm of the voltage divider consisted of a light-dependant resistor (LDR) as shown in Fig. 3. The other resistance (R) can be set according to the baseline light sensitivity of the wearer, thus fixing a base light attenuation level. Using a variable white light lamp, the intensity of the light incident on the photodetector was changed. For cross-polarizer configuration, when it is bright outside, the resistance of the LDR is low. Depending on the value of the baseline setting resistor, light can be attenuated accordingly. We measured the light intensity modulation performance of the artificial iris stack with TNCs made with 5CB and E7 nematic liquid crystal and with a commercial TNC (Boulder Vision). For target imaging, we placed a target image at a set distance from the artificial iris stack and maintained a constant illumination. We took images of the target using a commercial DSLR camera (Canon EOS 1200D) through a 4 mm aperture of the contact lens at different voltages provided through the LDR-based voltage divider.

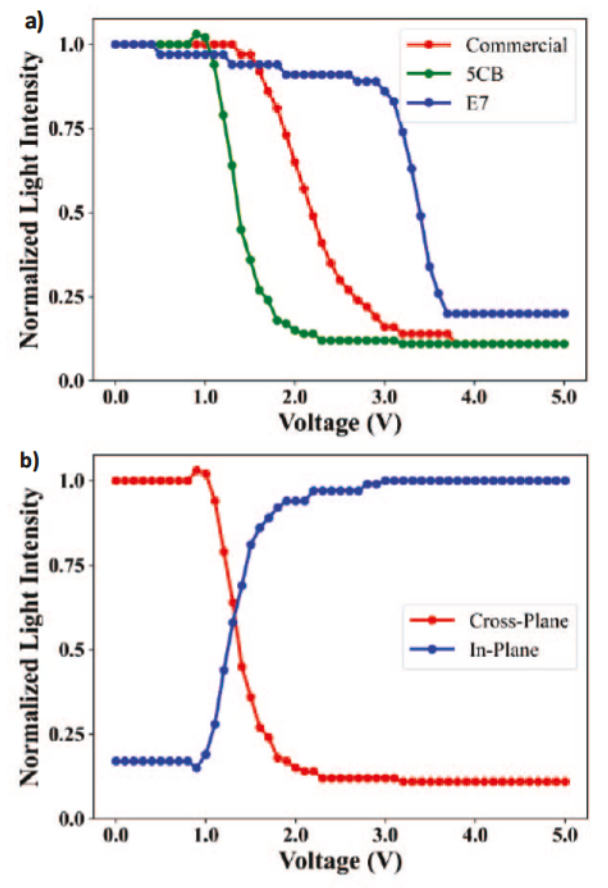


Fig. 4. Light attenuation performance of (a) Commercial, 5CB and E7-based TNC. (b) In-plane vs cross-plane polarizer configuration for 5CB-based TNC.

V. RESULTS AND DISCUSSIONS

Fig. 4. (a) shows the normalized attenuated light intensity for the commercial TNC and the TNCs made with 5CB and E7 liquid crystals. It can be observed that the TNC made with 5CB has a lower threshold voltage and covers the entire attenuation

range under 3.3 V, thus, making it suitable for use in low-power electronics. The attenuation range is also higher than that of the commercial TNC. Fig. 4. (b) shows the comparison of light attenuation in in-plane polarization and cross-plane polarization configuration. Cross-plane polarizer configuration can be utilized where a photophobic person spends the majority of their time in indoor conditions. Here without any voltage, maximum light is allowed to pass through. Conversely, the in-plane polarization configuration may be used in majorly outdoor conditions. This will result in the least power consumption. Fig. 5.a. shows target images for cross-plane polarization configuration when the iris is absent. Fig 5.b. to 5.d show represent an iris made with 5CB is present but no voltage is applied and 5CB iris when 1.5 and 2 V are applied. As observed, when iris is introduced, light is attenuated even if voltage is not applied. This reduction of light is equivalent to having a ND4 filter. When voltage is increased, the iris becomes darker. The maximum light attenuation is equivalent to having a ND32 fiter. A comparison of voltages required to be applied to the artificial iris in cross-plane configuration to achieve equivalent optical filter attenuation is shown in Table 1.

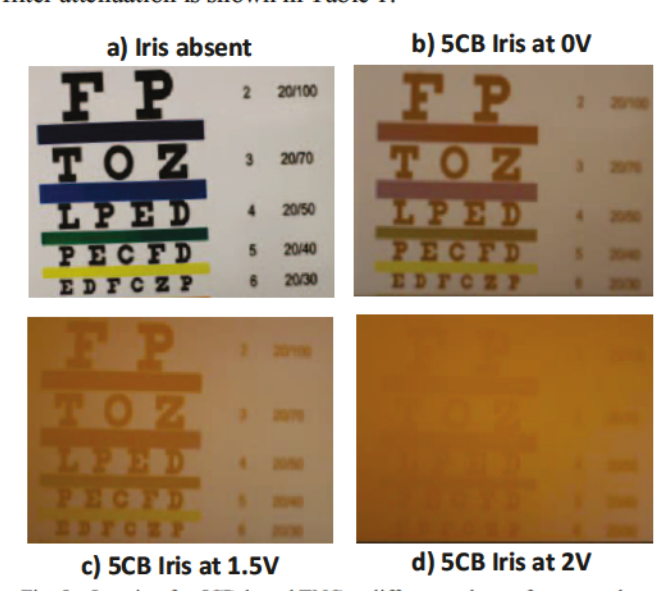


Fig. 5. Imaging for 5CB-based TNC at different voltages for cross-plane polarization.

TABLE I. APPLIED VOLTAGE VS EQUIVALENT OPTICAL ATTENUATION

Optical Filter	ND4	ND8	ND16	ND32
Voltage	0V	1.45V	1.65V	3.2V

VI. CONCLUSION

We demonstrated an artificial iris using twisted nematic cells on a smart contact lens platform with the ability to modulate the light intensity automatically using a LDR. Based on external lighting conditions and based on the wearer's sensitivity to light, a smart, automated system is built to deliver the appropriate amount of light to the user's eyes. It was shown that the fabricated iris stack has a lower threshold voltage than commercial one and an entire attenuation range (equivalent from ND4 to ND32) suited for 3.3V low-power systems. Further, the polarizer configuration can be modified to provide light attenuation in user-preferred indoor or outdoor environments.

REFERENCES

- J. E. Lebensohn and J. Bellows, "The Nature of Photophobia," Arch. Ophthalmol., vol. 12, no. 3, pp. 380–390, Sep. 1934.
- [2] Y. Wu and M. Hallett, "Photophobia in neurologic disorders," Translational Neurodegeneration, vol. 6, no. 1. BioMed Central Ltd., Sep. 20, 2017, doi: 10.1186/s40035-017-0095-3.
- [3] R. Noseda and R. Burstein, "Advances in understanding the mechanisms of migraine-type photophobia," Curr. Opin. Neurol., vol. 24, no. 3, pp. 197–202, Jun. 2011, doi: 10.1097/WCO.0b013e3283466c8e.
- [4] M. S. L. Robbins Richard B, "The Epidemiology of Primary Headache Disorders," Semin. Neurol., vol. 30, no. 02, pp. 107–119, 2010.
- [5] A. Albilali and E. Dilli, "Photophobia: When Light Hurts, a Review," Current Neurology and Neuroscience Reports, vol. 18, no. 9. Current Medicine Group LLC 1, Sep. 01, 2018, doi: 10.1007/s11910-018-0864-0.
- [6] H. Lee, R. Khan, and M. O'Keefe, "Aniridia: current pathology and management," Acta Ophthalmol., vol. 86, no. 7, pp. 708–715, Nov. 2008.
- [7] A. J. P. Vincent, E. L. H. Spierings, and H. B. Messinger, "A Controlled Study of Visual Symptoms and Eye Strain Factors in Chronic Headache," Headache J. Head Face Pain, vol. 29, no. 8, pp. 523–527, Sep. 1989.
- [8] B. J. Katz and K. B. Digre, "Diagnosis, pathophysiology, and treatment of photophobia," Survey of Ophthalmology, vol. 61, no. 4. Elsevier USA, pp. 466–477, Jul. 01, 2016, doi: 10.1016/j.survophthal.2016.02.001.
- [9] A. J. Wilkins, I. Nimmo-Smith, A. I. Slater, and L. Bedocs, "Fluorescent lighting, headaches and eyestrain," Light. Res. Technol., vol. 21, no. 1, pp. 11–18, Mar. 1989, doi: 10.1177/096032718902100102.
- [10] W. H. Adams, K. B. Digre, B. C. K. Patel, R. L. Anderson, J. E. A. Warner, and B. J. Katz, "The Evaluation of Light Sensitivity in Benign Essential Blepharospasm," Am. J. Ophthalmol., vol. 142, no. 1, pp. 82-87.e8, 2006, doi: https://doi.org/10.1016/j.ajo.2006.02.020.
- [11] D. Romano et al., "Artificial iris implantation in congenital aniridia A systematic review," Surv. Ophthalmol., 2022.
- [12] S. J. Vincent, "The use of contact lenses in low vision rehabilitation: optical and therapeutic applications," Clin. Exp. Optom., vol. 100, no. 5, pp. 513–521, Sep. 2017, doi: https://doi.org/10.1111/cxo.12562.
- [13] M. Rana, V. Savant, and J. I. Prydal, "A new customized artificial iris diaphragm for treatment of traumatic aniridia," Contact Lens Anterior Eye, vol. 36, no. 2, pp. 93–94, 2013.
- [14] A. Deshpande et al., "High-Toughness Aluminum-N-Doped Polysilicon Wiring for Flexible Electronics," in 2022 IEEE International Conference on Flexible and Printable Sensors and Systems (FLEPS), 2022, pp. 1–4, doi: 10.1109/FLEPS53764.2022.9781554.
- [15] A. Deshpande, E. Pourshaban, C. Ghosh, A. Banerjee, H. Kim, and C. Mastrangelo, "Adhesion Strength of PDMS to Polyimide Bonding with Thin-film Silicon Dioxide," in 2021 IEEE International Conference on Flexible and Printable Sensors and Systems (FLEPS), 2021, pp. 1–4, doi: 10.1109/FLEPS51544.2021.9469779.
- [16] A. Deshpande, M. U. Karkhanis, C. Ghosh, H. Kim, and C. H. Mastrangelo, "Ultralow Power Flexible Ocular Microsystem for Vergence and Distance Sensing Based on Passive Differential Magnetometry," in 2023 IEEE 36th International Conference on Micro Electro Mechanical Systems (MEMS), 2023, pp. 362–365, doi: 10.1109/MEMS49605.2023.10052200.

- [17] S. Kalidasan, C. Ghosh, A. P. Deshpande, C. H. Mastrangelo, and R. Walker, "Energy and Accuracy Characterization of a Burst-Mode Range Sensing Approach for Smart Contact Lenses," in 2022 IEEE Sensors, 2022, pp. 1–4, doi: 10.1109/SENSORS52175.2022.9967207.
- [18] A. Deshpande et al., "Ultralow Power On-the-Eye Vergence and Distance Sensing Through Differential Magnetometry," IEEE Access, vol. 11, pp. 28596–28609, 2023, doi: 10.1109/ACCESS.2023.3258918.
- [19] E. Pourshaban et al., "Flexible and Semi-Transparent Silicon Solar Cells as a Power Supply to Smart Contact Lenses," ACS Appl. Electron. Mater., vol. 4, no. 8, pp. 4016–4022, 2022, doi: 10.1021/acsaelm.2c00665.
- [20] E. Pourshaban et al., "Eye Tear Activated Mg-Air Battery Driven by Natural Eye Blinking for Smart Contact Lenses," Adv. Mater. Technol., vol. 8, no. 1, p. 2200518, 2023, doi: https://doi.org/10.1002/admt.202200518.
- [21] E. Pourshaban et al., "A Magnetically-Coupled Micromachined Electrostatic Energy Harvester Driven by Eye Blinking Motion," in 2021 21st International Conference on Solid-State Sensors, Actuators and Microsystems (Transducers), 2021, pp. 960–963, doi: 10.1109/Transducers50396.2021.9495499.
- [22] E. Pourshaban et al., "Flexible Electrostatic Energy Harvester Driven by Cyclic Eye Tear Wetting and Dewetting," in 2021 IEEE International Conference on Flexible and Printable Sensors and Systems (FLEPS), 2021, pp. 1–4, doi: 10.1109/FLEPS51544.2021.9469729.
- [23] E. Pourshaban, A. Banerjee, C. Ghosh, A. Deshpande, H. Kim, and C. H. Mastrangelo, "Semi-transparent and Flexible Single Crystalline Silicon Solar Cell," in 2021 IEEE 48th Photovoltaic Specialists Conference (PVSC), 2021, pp. 1897–1900, doi: 10.1109/PVSC43889.2021.9518571.
- [24] E. Pourshaban, M. U. Karkhanis, A. Deshpande, A. Banerjee, H. Kim, and C. H. Mastrangelo, "A Micro-Watt Electrolytic Power Scavenger driven by Eye-Blinking Motion," in 2021 IEEE Sensors, 2021, pp. 1–4, doi: 10.1109/SENSORS47087.2021.9639459.
- [25] A. Banerjee et al., "Microfabricated Low-Profile Tunable LC-Refractive Fresnel (LCRF) Lens for Smart Contacts," in Conference on Lasers and Electro-Optics, 2022, p. AW4C.3, doi: 10.1364/CLEO_AT.2022.AW4C.3.
- [26] A. Banerjee et al., "Microfabricated Low-Profile High Tunable LC Fresnel Lens for Smart Contacts," in 2022 IEEE Photonics Conference (IPC), 2022, pp. 1–2, doi: 10.1109/IPC53466.2022.9975691.
- [27] A. Banerjee et al., "Refractive-type varifocal liquid-crystal Fresnel lenses for smart contacts," Opt. Express, vol. 31, no. 10, pp. 17027–17049, 2023, doi: 10.1364/OE.489093.
- [28] A. Vásquez Quintero, P. Pérez-Merino, and H. De Smet, "Artificial iris performance for smart contact lens vision correction applications," Sci. Rep., vol. 10, no. 1, p. 14641, 2020, doi: 10.1038/s41598-020-71376-1.
- [29] M. F. Schiekel and K. Fahrenschon, "Deformation of Nematic Liquid Crystals with Vertical Orientation in Electrical Fields," Appl. Phys. Lett., vol. 19, no. 10, pp. 391–393, Nov. 1971, doi: 10.1063/1.1653743.
- [30] A. Safrani and I. Abdulhalim, "Liquid-crystal polarization rotator and a tunable polarizer," Opt. Lett., vol. 34, no. 12, pp. 1801–1803, 2009.
- [31] N. Konforti, E. Marom, and S. T. Wu, "Phase-only modulation with twisted nematic liquid-crystal spatial light modulators.," Opt. Lett., vol. 13 3, pp. 251–3, 1988.